Yields of Krypton Isotopes from the Deuteron and Alpha Bombardment of Heavy Nuclei*

MORTON KAPLAN† AND CHARLES D. CORYELL
Department of Chemistry and Laboratory for Nuclear Science, Massachusetts Institute of Technology, Cambridge, Massachusetts
(Received August 3, 1961)

The relative yields of 4.4-hr Kr^{85m}, 78-min Kr^{87}, and 2.8-hr Kr^{88} have been measured radiochemically for the fission of Th^{232}, U^{235}, and U^{238} induced by 14- and 9-Mev deuterons and 25-Mev alpha particles. Yields of these nuclides were also determined for the fission of U^{235} with thermal neutrons. By correcting for charge distribution, relative chain yields were obtained for mass numbers 85, 87, and 88. The results for thermal neutron fission of U^{235} are in good agreement with mass-spectrometrically determined yields at these mass numbers. Deviations from smooth yield-mass curves are found for deuteron fission of Th^{232} and alpha-particle fission of Th^{232}, U^{235}, and U^{238}, whereas deuteron fission of U^{235} and U^{238} show normal mass yields. The origin of these fine-structure effects is not understood, but no evidence has been found for a systematic influence of the 50-neutron shell in perturbing the fission yields in the krypton mass region.

I. INTRODUCTION

THE early radiochemical investigation of slow-neutron-induced fission indicated that the yields of fission product chains varied smoothly with mass number.[1] However, marked deviations from a smooth curve were definitely established by Thode and co-workers[2,3] in mass spectrometric determinations of the relative abundances of stable krypton and xenon isotopes produced in U^{235} fission and by Stanley and Katcoff[4] in radiochemical determinations of the yield of I^{136} in the fission of U^{233}, U^{235}, and Pu^{239}. Further work[5–12] has shown that the phenomenon of fine structure in the mass-yield curve is general for low-energy fission, and that this fine structure is related to the occurrence of closed nuclear shells.

In order to explain the observed fine structure, Glendenin[13] suggested, on the basis of binding-energy arguments, that fission fragments which, after emitting the usual number of prompt neutrons, are left with 51 or 83 neutrons might emit an extra neutron rather than the usual gamma rays. Pappas[14,15] extended this reasoning to closed-shell-plus-odd-neutron species, and Wiles[5] proposed that, in addition, fragments with closed shell configurations are favored in the fission act itself. One would expect the influence of closed shells to be greatest in the 82-neutron shell region because of the high fission yield of the species of interest, and a combination of the above arguments serves to satisfactorily explain the very pronounced fine structure observed in this region.[14] However, similar considerations applied to the region of the closed shell at 50 neutrons showed no agreement between the predicted and the experimentally determined fission yields of stable krypton isotopes.[11]

Considering all the available evidence concerning fine-structure effects, it would seem obvious that nuclear shell structure plays a significant role in the fission process.[16] However, the precise manner in which closed nuclear shells exert their influence is still far from being understood. It is particularly puzzling that the 82-neutron shell seems to have a much more direct effect than the similar shell at 50 neutrons. As yet no experimental evidence has been found which would indicate either a selectivity in the fission act or enhanced neutron emission from primary fragments due specifically to the inherent stability of the 50 neutron shell.

The present investigation was carried out in an attempt to examine more closely the influence of the 50-neutron shell in the fission process. As will be described in succeeding sections, the relative fission yields of Kr^{85m}, Kr^{87}, and Kr^{88} have been measured radiochemically for deuteron and alpha-particle induced fission of Th^{232}, U^{235}, and U^{238} at several bombarding energies. To facilitate comparison with published work

* This research is taken in part from the Ph.D. thesis submitted by M. Kaplan to the Department of Chemistry, January, 1960 (unpublished). The work has been supported by the U. S. Atomic Energy Commission.
† Present Address: Lawrence Radiation Laboratory, University of California, Berkeley 4, California.
[1] C. D. Coryell and N. Sugarman, *Radiochemical Studies: The Fission Products* (McGraw-Hill Book Company, Inc., New York, 1951), National Nuclear Energy Series, Plutonium Project Record, Vol. 9, Div. IV. See especially Part V.
[2] H. G. Thode and R. L. Graham, Can. J. Research **25A**, 1 (1947).
[3] J. Macnamara, C. B. Collins, and H. G. Thode, Phys. Rev. **78**, 129 (1950).
[4] C. W. Stanley and S. Katcoff, J. Chem. Phys. **17**, 653 (1949).
[5] D. R. Wiles, M. Sc. thesis in Chemistry, McMaster University, Hamilton, Canada, 1950 (unpublished).
[6] D. R. Wiles, B. W. Smith, R. Horsley, and H. G. Thode, Can. J. Phys. **31**, 419 (1953).
[7] L. E. Glendenin, E. P. Steinberg, M. G. Inghram, and D. C. Hess, Phys. Rev. **84**, 860 (1951).
[8] E. P. Steinberg and L. E. Glendenin, Phys. Rev. **95**, 431 (1954).
[9] E. P. Steinberg, L. E. Glendenin, M. G. Inghram, and R. J. Hayden, Phys. Rev. **95**, 867 (1954).
[10] R. K. Wanless and H. G. Thode, Can. J. Phys. **33**, 541 (1955).
[11] W. Fleming, R. H. Tomlinson, and H. G. Thode, Can. J. Phys. **32**, 522 (1954).
[12] J. A. Petruska, H. G. Thode, and R. H. Tomlinson, Can. J. Phys. **33**, 693 (1955).
[13] L. E. Glendenin, Ph.D. thesis in Chemistry, Massachusetts Institute of Technology, 1949 (unpublished); also Massachusetts Institute of Technology Laboratory for Nuclear Science Technical Report No. 35, 1949 (unpublished).
[14] A. C. Pappas, Massachusetts Institute of Technology Laboratory for Nuclear Science Technical Report No. 63, 1953 (unpublished).
[15] A. C. Pappas, Z. Elektrochem. **58**, 620 (1954).
[16] C. D. Coryell, Dedication U. S. Naval Radiological Defense Laboratory, San Francisco, California, August, 1957.

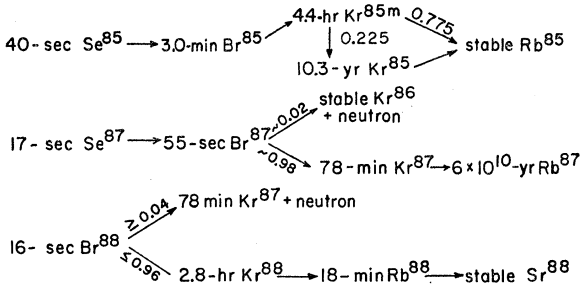

FIG. 1. Fission product decay chains for mass numbers 85, 87, and 88.

the yields of these nuclides were also measured for the fission of U^{235} with thermal neutrons.

The fission-product decay chains which were studied in this work are shown[17] in Fig. 1. As can be seen, measurements of the fission yields of the krypton isotopes will give values for the cumulative yields of the respective mass chains up to $Z=36$ (krypton), provided sufficient time has elapsed to permit the complete decay of all short-lived precursors. Small corrections were made for the expected yields of isobars of $Z>36$ to obtain total cumulative yields of the three mass chains. Fine structure information is sought by comparison of these chain yields with one another (eliminating problems of absolute calibration), and with existing information for neighboring mass numbers, based principally on radiochemical data for Br^{83}, Br^{84}, and Sr^{89}. The correlations are assisted by the fact that the logarithm of the chain yield is approximately linear with mass number in this region. It was decided to choose mass number 88 as the point of normalization, since on theoretical grounds shell effects would be least likely to be found here.

II. EXPERIMENTAL

A. Irradiations and Chemistry

For the experiments with U^{238} and Th^{232}, the targets consisted of small natural uranium foils (35.7 mg/cm^2) and natural thorium foils (70.9 mg/cm^2) obtained from Metals and Controls, Inc., Attleboro, Massachusetts. The U^{235} runs were made using powdered samples of U_3O_8 highly enriched in U^{235}, furnished by the United States Atomic Energy Commission. The isotopic composition as determined by mass spectrometric analysis was: U^{235}, 93.14%; U^{234}, 0.96%; U^{236}, 0.33%; U^{238}, 5.57%.

In the deuteron and alpha runs, the appropriate target was wrapped in a single thickness of thin (1.88 mg/cm^2) aluminum foil and irradiated in the external beam of the M.I.T. cyclotron. The bombardment times ranged from 10 sec to several minutes, depending on the reaction being studied and the beam current available. The average energy of the beam striking the fissile target was computed from the range-energy curves of Rich and Madey[18] to be 14.0 Mev for the deuteron bombardments and 25.5 Mev for the alpha-particle bombardments. In experiments to be carried out at lower energy, the deuteron beam was degraded to 9.3 Mev with aluminum absorbers.

The calculated beam energy loss in the targets themselves varies from 0.6 Mev for 14.0-Mev deuterons incident on the natural uranium foil to 5 Mev for 25.5-Mev alpha particles incident on the thorium target foils. Consequently, there is some uncertainty in the average energy causing fission in the targets. However, as the relative fission yields in the mass region of interest (the slope of the light wing of the light-mass peak) change only very slowly with energy in this energy range,[19,20] the distribution of energies across the target will not have a serious effect on the results of the measurements. For convenience in discussing the various experiments, we shall refer to the irradiations by the beam energy incident upon the target surface.

The experiments on thermal neutron fission of U^{235} were carried out with samples which had received short irradiations in the rapid removal facility of the M.I.T. reactor.

About 20 min after irradiation, the target material and its aluminum wrapper were dissolved in an appropriate solvent in a gas-handling system designed for these experiments. (The solvents employed were: uranium foil targets, 10 ml conc. HCl plus 1 ml conc. HNO_3; thorium foil targets, 10 ml conc. HCl plus 10 mg NaF; U_3O_8 targets, 5 ml conc. HCl followed by 5 ml conc. HNO_3. In all cases, after dissolution was complete the target solution was diluted by the addition of 5 ml H_2O.) The volatile components were swept from solution by a stream of helium flowing through the system for about 10 min. The bulk of the water and acid vapors and some of the fission-produced halogens were extracted from the gas stream by means of NaOH pellets, and the remaining non-noble gas impurities were removed by passage over a hot (900°C) titanium getter. The krypton and xenon were finally collected by adsorption on charcoal at liquid nitrogen temperature, and separated from each other by means of a two-stage, temperature-regulated, charcoal adsorption trap.

Preliminary studies were carried out to determine the optimum conditions for effecting a rapid and clean separation of krypton in the system. Provision was made for the injection of measured quantities of non-radioactive krypton and xenon carriers to facilitate the purification process. However, it was found that equally good results were obtained when the procedure was carried through using only the helium transport gas and consequently, the addition of isotopic carriers was omitted. No measurements were made of the over-all efficiency of the krypton recovery, but a rough estimate of the chemical yield would be of the order

[17] S. Katcoff, Nucleonics **18**, No. 11, 201 (1960).
[18] M. Rich and R. Madey, University of California Radiation Laboratory Report UCRL-2301, Berkeley, 1954 (unpublished).
[19] T. T. Sugihara, P. J. Drevinsky, E. J. Troianello, and J. M. Alexander, Phys. Rev. **108**, 1264 (1957).
[20] R. Gunnink and J. W. Cobble, Phys. Rev. **115**, 1247 (1959).

of 50%. The krypton samples obtained in this way were found to be free of any detectable radioactive contamination, as shown by the absence of 9.2-hr Xe^{135} and 5.3-day Xe^{133}.

The counting of the krypton samples was carried out with a β-proportional counter designed and constructed in a manner conventional for gas-phase counting. The krypton was transferred in vacuum from the charcoal trap to the evacuated counter by means of a Toepler pump. A counting gas mixture of 90% argon and 10% methane was then admitted via a device which filled the counter to atmospheric pressure, and the counter was isolated from the remainder of the apparatus. Counting rate measurements were usually begun between 60 and 90 min after the end of the target irradiation. When necessary, small, empirically determined corrections were applied to the counting data to account for dead-time losses.

B. Analysis of Decay Curves

Reference to Fig. 1 shows that at a short time after counting is begun, the species which will contribute to the observed counting rate are 4.4-hr Kr^{85m}, 78-min (=1.3-hr) Kr^{87}, 2.8-hr Kr^{88}, and its daughter product 18-min Rb^{88}. The Kr^{85} ground state (half-life 10.3 yr) is so long-lived that its contribution is much too small to be detected. Krypton isotopes of mass numbers greater than 88 are too short-lived to have survived the duration of the chemical purification procedure.

The resolution of a multicomponent decay curve containing species of similar half-life requires specialized techniques. We were able to take advantage of the fact that an independent measurement of the Rb^{88} activity grown in by decay of the parent Kr^{88} could be used to calculate the contribution of Kr^{88} to the total observed activity. The chemical separation is based on the fact that a newly formed Rb^{88} ion, produced by the decay of a Kr^{88} atom, finds itself in an intense electric field (in the counter) and being positively charged it is accelerated to the counter wall and remains there. Consequently, the krypton may be removed from the rubidium very rapidly and very efficiently by opening a valve connecting the counter to the vacuum pumps. The counter may then be refilled with fresh counting gas and the Rb^{88}, being already present, may be counted. (Repeated pumping and refilling of the counter showed no change in the Rb^{88} activity, except for radioactive decay.)

The procedure employed in our experiments was as follows. The decay of the krypton sample was followed for a time sufficiently long to give a workable decay curve. This time was considerably longer than that necessary to establish radioactive equilibrium between Kr^{88} and Rb^{88}. During this period of observation (a minimum of four hours), approximately one hundred counting-rate measurements were taken. The krypton was then removed by pumping, the counter was refilled with counting gas, and the Rb^{88} counting rate

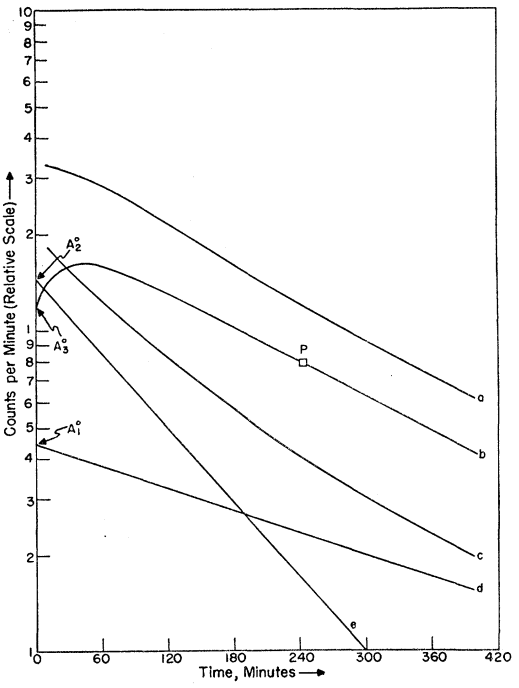

FIG. 2. Analysis of krypton decay curve. (a) is the experimentally obtained decay curve corrected for background and counter deadtime. (b) is the synthetic $Kr^{88}-Rb^{88}$ decay curve constructed to pass through the fixed point P, the $Kr^{88}+Rb^{88}$ contribution at the time of the Kr-Rb separation. (c) is curve (b) subtracted from curve (a). (d) is the contribution of Kr^{85m} and (e) is the contribution of Kr^{87}, both obtained by resolution of curve (c).

determined. The Rb^{88} measurements were begun three to four minutes after the separation of the parent, and were continued over several half-lives. From the counting rate of Rb^{88} at the time of separation, the contribution of Kr^{88} to the total observed counting rate (at this time) was computed from the relation:

$$A_3/A_4=(C_3/C_4)(\lambda_4-\lambda_3)/\lambda_4, \quad (1)$$

where A_3 and A_4 are the counting rates of Kr^{88} and Rb^{88}, respectively, C_3/C_4 is the counting efficiency of Kr^{88} relative to that of Rb^{88}, and λ_3 and λ_4 are the respective decay constants. The calculation of counting efficiencies discussed in Appendix I gave $C_3/C_4=1.000/0.785$.

A synthetic Kr^{88}-Rb^{88} decay curve was then used to subtract the contribution of these species from the observed total decay curve. The synthetic decay curve was constructed from the general relationship:

$$A_{3+4}=C_3A_3{}^0\exp(-\lambda_3 t)+\frac{C_4\lambda_4A_3{}^0}{\lambda_4-\lambda_3}[\exp(-\lambda_3 t)-\exp(-\lambda_4 t)], \quad (2)$$

where A_{3+4} is the activity of $Kr^{88}+Rb^{88}$, C_3 and C_4 are their counting efficiencies, and $A_3{}^0$ is a constant fixed by the requirement that A_{3+4} be equal to the computed counting rate of $Kr^{88}+Rb^{88}$ at t equal to the time of the krypton-rubidium separation.

The curve obtained by subtraction of the mass 88

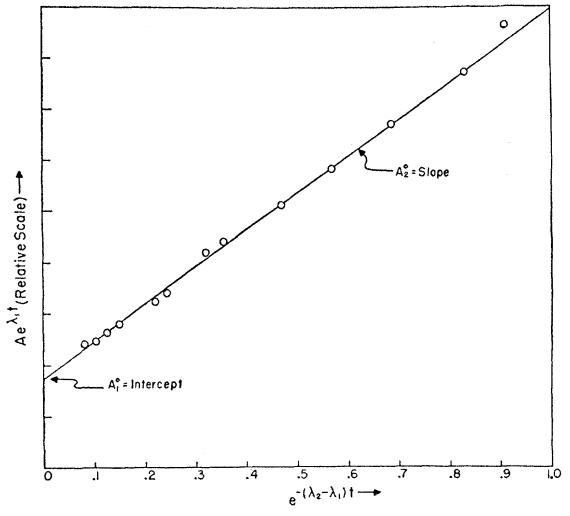

FIG. 3. Resolution of Kr^{85m} and Kr^{87}.

contribution from the total decay curve represents only the decay of 4.4-hr Kr^{85m} and 78-min Kr^{87}:

$$A(t)=A_1^0\exp(-\lambda_1 t)+A_2^0\exp(-\lambda_2 t), \qquad (3)$$

where A_1^0 and A_2^0 are the counting rates of species 1 and 2, respectively, at time $t=0$. Equation (3) may be rewritten in the form:

$$A(t)\exp(\lambda_1 t)=A_1^0+A_2^0\exp[-(\lambda_2-\lambda_1)t], \qquad (4)$$

to show that a plot of $A(t)\exp(\lambda_1 t)$ vs $\exp[-(\lambda_2-\lambda_1)t]$ gives a straight line with ordinate intercept A_1^0 and slope A_2^0. This type of expanded plot gives a greater accuracy than ordinary graphical subtraction, and yielded the values of A_1^0 and A_2^0 needed to determine the contributions of Kr^{85m} and Kr^{87}, respectively.

Figure 2 shows the completed analysis of the total decay curve into its components. In the figure, curve (a) is the experimentally obtained decay curve, corrected for background and counter deadtime. Curve (b) is the synthetic Kr^{88}-Rb^{88} decay curve constructed to pass through the fixed point P, the $Kr^{88}+Rb^{88}$ contribution at the time of the krypton-rubidium separation. Curve (c) is obtained by subtraction of curve (b) from curve (a). Curves (d) and (e) represent the contributions of Kr^{85m} and Kr^{87}, respectively, which result from the resolution of curve (c). The latter resolution, by the method of Eq. (4), is shown in Fig. 3. The intercepts of curves (d), (e), and (b) (Fig. 2) on the ordinate axis ($t=0$) represent the counting rates of Kr^{85m}, Kr^{87}, and Kr^{88} (denoted A_1^0, A_2^0, and A_3^0), respectively, at the time of the beginning of counting.

This method of analysis of the decay curves was found to give consistent results, the separated components decaying in the proper manner and with half-lives in excellent agreement with the known values.

In some experiments, the krypton-rubidium separation was not carried out but instead the decay of the krypton sample was followed for an extended period of time. This was done in order to check that the samples were free of xenon activity, and also to verify that the method of decay curve analysis would work equally well over longer time intervals. In these experiments (Figs. 2 and 3 are of this type), the fixed point giving the mass 88 contribution was obtained from separate duplicate experiments in which the krypton-rubidium separation was made. This procedure is justified by the fact that the ratio of the Kr^{88} counting rate to the total counting rate is the same in duplicate experiments, at a given time after irradiation. These experiments verified the consistency of the method employed for decay curve analysis, and also showed the krypton samples to be free of xenon contamination.

TABLE I. Decay constants and corresponding half-lives used in this work.

Nuclide	Decay constant	Half-life
Kr^{85m}	0.00262 min^{-1}	4.40 hr
Kr^{87}	0.00889 min^{-1}	78.0 min
Kr^{88}	0.00412 min^{-1}	2.80 hr
Rb^{88}	0.03915 min^{-1}	17.7 min

In the above analysis we have not included perturbations that could arise from 1.9-hr Kr^{83m}, descended[17] from 2.3-hr Br^{83} and in part from 25-min Se^{83}. It is expected that its contribution is very small because of the much lower fission yield at mass 83 and the large holdup of chain 83 in the form of precursors of Kr^{83m} during the time to krypton separation. Calculations show that at the time of counting the contribution of Kr^{83m} would be at most 3% of the initial counting rate (using the flattest yield-mass curve found and the longest time before separation was complete). The method of analysis attributes the Kr^{83m} activity to Kr^{85m} and Kr^{87}, with upper limits of the contribution being 2 and 4%. Since these limits are comparable with the experimental error in the A^0 values, and no direct evidence for Kr^{83m} was seen in any decay curve component, we have neglected the effects of Kr^{83m}.

In performing the various analyses and other calculations which were necessary in this work, one must have an accurate knowledge of the decay constants (λ's) or corresponding half-lives of the nuclides of interest. As these quantities are not known to better than a few per cent, a set of values was chosen and used consistently throughout. For convenience, these selected constants are presented together in Table I. They are in good agreement with the values given by Katcoff.[17]

III. RESULTS

A. General Considerations

The analysis of the krypton decay curves provides counting rates for Kr^{85m}, Kr^{87}, and Kr^{88} at a time t after the target irradiation. In order to determine the relative disintegration rates, we must have a knowledge of the fraction of the disintegrations of each nuclide which are actually counted. No corrections for absorption of the radiations need be considered, as the

samples are in the gas phase within the counter. The number of krypton atoms of a given nuclear species which happens to be located in the small insensitive volume of the counter will be proportional to the total number of atoms of that species present, and consequently will not affect the relative measurements. In addition, the amplification of the counting system is sufficiently high so that the fraction of the pulses which are too small to pass the scaling circuit discriminator (arising from the low-energy end of the β-ray spectrum) is negligible. On the basis of these arguments, we define the counting efficiency of the krypton isotopes decaying by β emission to be 1.000.

The decay Kr^{87} and of Kr^{88} proceed only by β emission, and hence their relative disintegration rates can be taken as being equal to their counting rates. However, in the case of Kr^{85m}, 77.5% of the decays proceed by β emission to Rb^{85} and 22.5% by isomeric transition to the Kr^{85} ground state.[21] The isomeric transition is appreciably internally converted,[21] and the internal conversion electrons will have been counted as efficiently as β rays. Calculations based upon these considerations are given in Appendix I, with the result that the relative disintegration rate of Kr^{85m} is equal to its counting rate multiplied by the factor 1.19.

Once the relative disintegration rates of the species of interest have been determined at a known time after the target irradiation, the relative formation cross sections for these species may be computed in the usual way. As all short-lived precursors would have decayed away by the time krypton was separated from the target, we have, for convenience, carried out the calculations as though the krypton isotopes were formed directly in the irradiation.

The total chain fission yields for each mass number were obtained from the formation cross sections for the krypton isotopes by correcting for the independent production in fission of chain members with atomic numbers greater than 36. These corrections require a knowledge of the distribution of nuclear charge along a given mass chain. As the charge distribution varies with the compound nucleus undergoing fission, as well as with the excitation energy involved, we must be able to compute appropriate corrections for each of the different fission reactions studied in our work. The study of charge distribution has been carried out most thoroughly for the fission of U^{235} with thermal neutrons. Unfortunately, charge distribution data are scarce for many of the other fission reactions studied here. In view of these circumstances, a semiempirical method was developed[22] whereby the distribution of nuclear charge to be expected in the fission reactions of interest could be obtained from the known charge distribution for thermal neutron fission of U^{235}. For a given fission reaction, the corrections are greatest for the mass 88 chain and least for the mass 85 chain. The largest correction applied was for the mass 88 chain in the fission of U^{235} with 14-Mev deuterons, and amounted to 17% of the total chain yield. In general, however, the corrections were much smaller, ranging from less than 0.1% to several percent. Variations in the method of computing the charge distribution corrections would yield results not very different from our own.

As a final point, the charge distribution calculations were used to estimate the independent yield of 10.3-yr Kr^{85} (not detectable in our measurements), and a very small correction was made for this effect.

In the following sections the experimental results are presented, and for convenience the different fission reactions investigated are discussed separately.

B. Deuteron Bombardments

The results obtained in the studies of deuteron-induced fission are given in Table II. The first two columns in the table show the irradiation number and the fission reaction, respectively. The subscript on the d indicates the deuteron energy incident upon the target material. The third column gives the ratio of the formation cross section for Kr^{85m} to that for Kr^{88}, denoted by σ_{85}/σ_{88}. These ratios were calculated directly from the experimental measurements (after analysis of the decay curves), and include the appropriate counting efficiency factors. The fourth column gives the ratio of the total mass 85 chain yield to that of mass 88, denoted by Y_{85}/Y_{88}. The ratios in this column were obtained from those in column 3 by application of the appropriate charge distribution corrections. Column 5 gives the average value of Y_{85}/Y_{88} from the duplicate experiments. The indicated uncertainty in this average value is the standard deviation of the mean (standard error) and is not intended to represent an absolute error estimation. Columns 6, 7, and 8 correspond to columns 3, 4, and 5, respectively, for the mass 87 to mass 88 ratios.

It has been shown by Sugihara *et al.*[19] that in the bombardment of natural uranium with 13.6- and 9.9-Mev deuterons, the fraction of the fissions which are caused by the fast neutron background is negligible. We expect the same to be true in our studies of deuteron-induced fission.

U^{238}

Six experiments were performed using natural uranium targets, four at an incident deuteron energy of 14.0 Mev and two at 9.3 Mev. The fission of natural uranium with deuterons has been studied by Sugihara *et al.*[19] at 13.6, 9.9, and 5.2 Mev, by Alexander and Coryell[23] at the same energies, and by Douthett and Templeton[24] at 18 Mev. Portions of the yield-mass curves obtained by Sugihara *et al.* at 13.6

[21] D. Strominger, J. M. Hollander, and G. T. Seaborg, Revs. Modern Phys. **30**, 585 (1958).

[22] C. D. Coryell, M. Kaplan, and R. D. Fink, Can. J. Chem. **39**, 646 (1961). In particular, see Appendix II of this reference.

[23] J. M. Alexander and C. D. Coryell, Phys. Rev. **108**, 1274 (1957).

[24] E. M. Douthett and D. H. Templeton, Phys. Rev. **94**, 128 (1954).

TABLE II. Experimental results for deuteron-induced fission. The subscript on the d indicates the incident deuteron energy in Mev.

Irradiation No.	Fission reaction	$(\sigma_{85}/\sigma_{88})^a$	$(Y_{85}/Y_{88})^b$	Average	$(\sigma_{87}/\sigma_{88})^a$	$(Y_{87}/Y_{88})^b$	Average
13	$U^{238}(d_{14},F)$	0.564	0.538		0.945	0.902	
14	$U^{238}(d_{14},F)$	0.592	0.564	0.552±0.006	0.911	0.869	0.878±0.013
15	$U^{238}(d_{14},F)$	0.587	0.560		0.886	0.845	
37	$U^{238}(d_{14},F)$	0.574	0.547		0.940	0.897	
43	$U^{238}(d_{9},F)$	0.552	0.542	0.547±0.005	0.930	0.913	0.921±0.009
50	$U^{238}(d_{9},F)$	0.563	0.552		0.948	0.930	
22	$Th^{232}(d_{14},F)$	0.650	0.614		1.014	0.958	
23	$Th^{232}(d_{14},F)$	0.641	0.605		1.007	0.952	
25	$Th^{232}(d_{14},F)$	0.653	0.617	0.643±0.019	0.932	0.880	0.903±0.024
38	$Th^{232}(d_{14},F)$	0.721	0.681		0.878	0.830	
55	$Th^{232}(d_{14},F)$	0.738	0.697		0.944	0.893	
44	$Th^{232}(d_{9},F)$	0.682	0.663		1.018	0.990	
51	$Th^{232}(d_{9},F)$	0.620	0.602	0.649±0.024	0.900	0.875	0.941±0.034
56	$Th^{232}(d_{9},F)$	0.702	0.681		0.986	0.959	
28	$U^{235}(d_{14},F)$	0.617	0.527	0.534±0.008	0.884	0.791	0.797±0.007
30	$U^{235}(d_{14},F)$	0.634	0.542		0.899	0.804	
45	$U^{235}(d_{9},F)$	0.577	0.519	0.488±0.031	0.898	0.828	0.710±0.118
54	$U^{235}(d_{9},F)$	0.509	0.458		0.643	0.593	

[a] Krypton formation cross-section ratios.
[b] Total mass chain-yield ratios.

and 9.9 Mev are shown in Fig. 4. Included also are the data reported by Alexander and Coryell at the same energies. Our experimental results have been normalized to the smoothly-drawn curves[19] at mass number 88 and the resulting fission yields for mass numbers 85 and 87 are indicated by circles.

As can be seen, the fission yields at mass numbers 85 and 87 agree quite well with the smooth yield-mass curves. No obvious deviations can be said to exist at either deuteron energy over the mass range 84 to 91.

Th^{232}

Eight deuteron bombardments were carried out with thorium foils, five at 14.0 Mev and three at 9.3 Mev. The only data available for comparison in this mass region are those of Alexander and Coryell[23] for 2.3-hr Br^{83}, 32-min Br^{84} (one value), and 51-day Sr^{89}, hardly enough to outline the yield-mass curve in this region. Figure 5 shows these data plotted as logarithm of relative yield vs. mass number. Assuming the validity of a linear relationship, the relative yield for $A=88$ is computed as 0.83. Our data for 14-Mev deuterons are normalized to this point. The points for Kr^{85m} and Kr^{87} lie above the line by 10 and 7%, respectively.

If appreciable curvature (concave downwards) is expected for the logarithm of yields vs mass number, the departure of the points for Kr^{85m} and Kr^{87} is reduced. Using the smooth curve drawn schematically by Alexander and Coryell,[23] the points for Kr^{85m} and Kr^{87} would not show departures larger than the uncertainty in their relative yield values.

There are no data at all in the literature for the deuteron fission of thorium at an energy near 9 Mev. In order to evaluate our results, we have assumed that in our mass range the curve for logarithm of yield vs mass number for deuteron fission of Th^{232} varies with energy in the same way as the curve[19] for U^{238}. As the

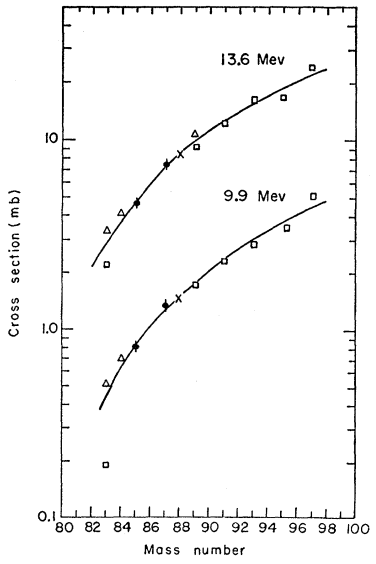

FIG. 4. Yield-mass curves for deuteron fission of U^{238}. □ Data of Sugihara *et al.* △ Data of Alexander and Coryell. × Point of normalization. ● This work.

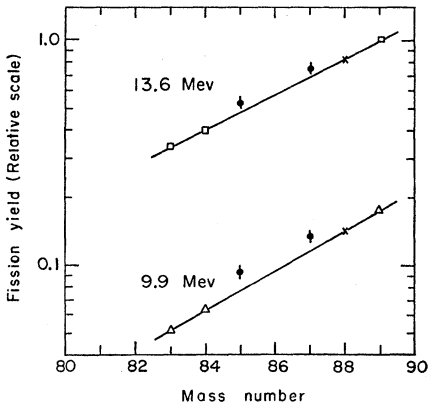

FIG. 5. Yield-mass curves for deuteron fission of Th^{232}. □ Data of Alexander and Coryell. △ Extrapolated data. × Point of normalization. ● This work.

TABLE III. Experimental results for alpha-particle induced fission. The subscript on the α indicates the incident α-particle energy in Mev.

Irradiation No.	Fission reaction	$(\sigma_{85}/\sigma_{88})^a$	$(Y_{85}/Y_{88})^b$	Average	$(\sigma_{87}/\sigma_{88})^a$	$(Y_{87}/Y_{88})^b$	Average
34	$U^{235}(\alpha_{,25},F)$	0.742	0.642	0.596±0.046	1.022	0.903	0.920±0.018
42	$U^{235}(\alpha_{25},F)$	0.635	0.550		1.039	0.938	
32	$U^{238}(\alpha_{25},F)$	0.621	0.592	0.576±0.016	1.023	0.975	0.942±0.033
39	$U^{238}(\alpha_{25},F)$	0.587	0.560		0.954	0.910	
33	$Th^{232}(\alpha_{25},F)$	0.591	0.558	0.553±0.004	0.942	0.890	0.869±0.011
41	$Th^{232}(\alpha_{25},F)$	0.578	0.546		0.916	0.865	
57	$Th^{232}(\alpha_{25},F)$	0.586	0.555		0.902	0.852	

[a] Krypton formation cross-section ratios.
[b] Total mass chain-yield ratios.

mass range is small and the energy interval not very large, this is probably a fair assumption. On this basis, the points shown as triangles in the lower half of Fig. 5 were computed and the smooth curve drawn. The results of our measurements were as usual normalized at mass number 88 and are shown as circles. Both the mass 85 and mass 87 yields lie considerably above the curve, the deviations being 21% for the former and 15% for the latter. It seems unlikely that curvature would remove more than half of the deviation.

If our thorium data may be interpreted as reflecting a real fine-structure effect, then one might expect such an effect to be more prominent at lower energies, in agreement with the relative deviations from the smooth curves for the 14.0- and 9.3-Mev experiments.

U^{235}

Four runs were made using targets of U_3O_8 highly enriched in U^{235}. Two of these were 14.0-Mev deuteron bombardments and the other two were at 9.3 Mev. The fission of U^{235} with 13.6-Mev deuterons has recently been studied by del Marmol.[25] The results of his fission-yield measurements at mass numbers 83, 84, and 89 are shown in Fig. 6. Included also is the fission yield of the mass 92 chain, obtained by reflection through the center of the yield-mass curve. The mass-yield ratios determined in the present work were again normalized at mass number 88 and the resulting fission yields for the mass 85 and mass 87 chains are shown as circles. These yields are in excellent agreement with the smooth curve drawn through del Marmol's points, and no deviations from this curve are visible.

As no fission yield curve is available for comparing our data at 9.3 Mev, we have followed the same procedure as in the case of Th^{232} discussed above. Using the energy variation of the fission yields for U^{238}, as obtained from Fig. 4, and del Marmol's results for U^{235} at 13.6 Mev, we have calculated the fission yields shown as triangles in the lower half of Fig. 6. Our results at 9.3 Mev, after normalization at mass number 88, are in agreement with the smooth yield-mass curve within the precision of the duplicate experiments.

[25] P. del Marmol, Ph.D. thesis, Department of Chemistry, Massachusetts Institute of Technology, Cambridge, Massachusetts, January, 1959 (unpublished).

C. Alpha-Particle Bombardments

Table III gives the results obtained for the alpha-particle induced fission reactions at 25.5 Mev. The various column headings are the same as those in Table II for deuteron bombardments. Two duplicate irradiations were carried out on the U^{235} and U^{238} targets and three runs were made with Th^{232}.

The fission of U^{235} with alpha particles has been investigated by several workers. Fairly complete yield-mass curves were obtained by Gunnink and Cobble[20] at six energies from 20 to 40 Mev. Figure 7(a) gives the yield-mass curve obtained by interpolation to 25 Mev. The mass-yield ratios determined in the present work have been normalized to the curve at mass number 88, and are indicated by circles. The fission yield for mass 85 agrees with the smooth curve within the experimental precision of the measurements. At mass number 87, our result falls above the curve by 8%, a discrepancy which is appreciably larger than the average deviation of the two duplicate runs.

In the cases of U^{238} and Th^{232}, there are no reliable data available with which to compare our results. The fission of U^{238} with alpha particles has been studied by

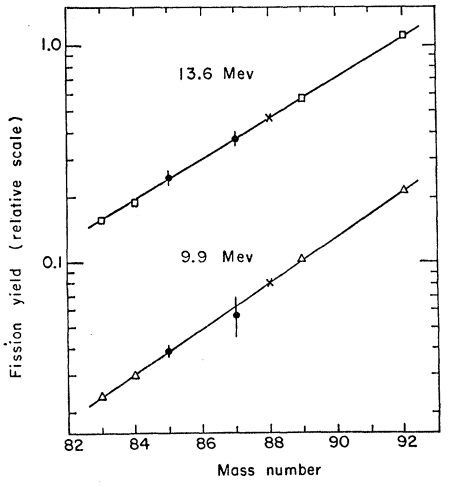

FIG. 6. Yield-mass curves for deuteron fission of U^{235}. □ Data of del Marmol. △ Extrapolated data. ✕ Point of normalization. ● This work.

TABLE IV. Experimental results for thermal-neutron induced fission of U^{235}.

Irradiation No.	$(\sigma_{85}/\sigma_{88})^a$	$(Y_{85}/Y_{88})^b$	Average	$(\sigma_{87}/\sigma_{88})^a$	$(Y_{87}/Y_{88})^b$	Average
40	0.426	0.425	0.386±0.025	0.634	0.633	0.659±0.013
49	0.405	0.404		0.674	0.673	
52	0.403	0.402		0.642	0.641	
58	0.315	0.314		0.691	0.690	

[a] Krypton formation cross-section ratios.
[b] Total mass chain-yield ratios.

Ritsema[26] over the energy range 22–45 Mev, and by Colby *et al.*[27] from 20 to 40 Mev. However, in the energy and mass regions of interest here, the yield-mass curves are not well defined, except to indicate that the logarithm of the fission yield is very roughly linear with mass number. The recent work of Chu[28] on fission yields in the rare-earth region, which is complementary to the mass region studied here, also indicates that a straight line approximation is valid in the mass range 84–88. Consequently, in Fig. 7(b) we have plotted our mass yield results for U^{238} on a relative scale by means of the normalization $Y_{88}=1.000$. The dashed line is drawn through the mass 85 and 87 points simply to show that the three values do not lie on a straight line. Expressed in this way, the mass 88 chain yield is low (or masses 85 and 87 are high) by 17%.

The alpha-particle induced fission of Th^{232} has been studied by Newton[29] at 37.5 Mev and by Foreman[30] in the energy range 15–46 Mev. The bombarding energy used by Newton is considerably higher than that employed in this study and it does not seem wise to attempt an extrapolation of Newton's fission-yield curve over so large an energy interval. The low-energy fission-yield data reported by Foreman contain uncertainties of 50% for his three yield measurements in the mass range 77–91. We have, therefore, employed the procedure used for the $U^{238}(\alpha,F)$ results, taking $Y_{88}=1.000$. The results so obtained are shown in Fig. 7(c). The line through the points for mass numbers 85 and 87 predicts a value for mass 88 which is 10% high.

The lines in Figs. 7(b) and 7(c) have higher slopes than given by the increments in logarithm of yields in the smooth curves of Figs. 4 through 7(a) for masses 85 to 88. This suggests not only a positive deviation at $A=87$ but one at $A=85$, relative to $A=88$.

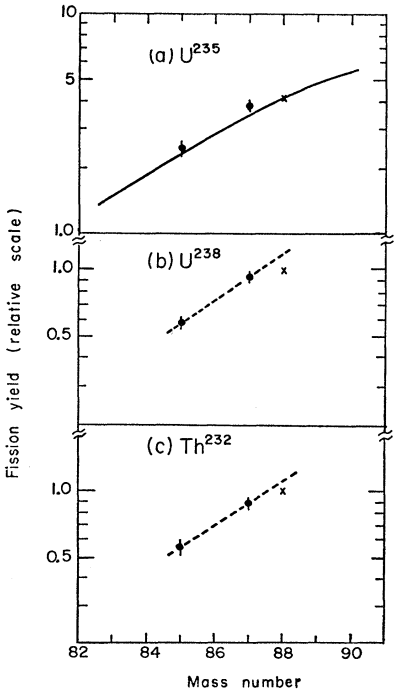

FIG. 7. Experimental results for fission induced by 25.5-Mev alpha particles. (a) U^{235}, (b) U^{238}, (c) Th^{232}. Solid line is the yield-mass curve obtained from the data of Gunnink and Cobble. Dashed lines show deviation of fission yields from a linear relationship. × Point of normalization. ● This work.

D. Thermal Neutron Bombardments

Four experiments were performed in which the mass-yield ratios were measured for the thermal neutron fission of U^{235}. The results of these experiments are given in Table IV. As before, the krypton formation cross-section ratios are given first, followed by the total mass-yield ratios.

The equivalent of our σ ratios has been measured by Koch *et al.*[31] These authors extracted the noble gas fraction from an irradiated uranium oxide target, and by means of a mass spectrometer were able to separate the various krypton isotopes according to mass. The isolated samples were then assayed by β counting and relative formation cross sections were calculated for Kr^{85m}, Kr^{87}, and Kr^{88}. The results reported as the average of two duplicate experiments were $\sigma_{85}/\sigma_{88}=0.33\pm0.10$ and $\sigma_{87}/\sigma_{88}=0.70\pm0.15$. In arriving at these values, no allowance was made for the isomeric transition branch in the decay of Kr^{85m}, and if we apply a correction to account for this effect, their value for σ_{85}/σ_{88} becomes 0.39 ± 0.12. These cross-section ratios agree quite well with our results in Table IV.

The best mass-yield data available for the thermal

[26] S. E. Ritsema, University of California Radiation Laboratory Report UCRL-3266, Berkeley, 1956 (unpublished).
[27] L. J. Colby, Jr., M. L. Shoaf, and J. W. Cobble, Phys. Rev. 121, 1415 (1961).
[28] Y. Y. Chu, University of California Radiation Laboratory Report UCRL-8926, Berkeley, 1959 (unpublished).
[29] A. S. Newton, Phys. Rev. 75, 17 (1949).
[30] B. M. Foreman, University of California Radiation Laboratory Report UCRL-8223, Berkeley, 1958 (unpublished).
[31] J. Koch, O. Kofoed-Hansen, P. Kristensen, and W. Drost-Hansen, Phys. Rev. 76, 279 (1949).

TABLE V. Comparison of chain yields with smooth Yield-mass curves.[a]

Fission reaction[b]	Deviation at mass 85 (%)	Deviation at mass 87 (%)
$U^{238}+d_{14}$	0	0
$U^{238}+d_9$	0	0
$Th^{232}+d_{14}$	0 to 10	0 to 7
$Th^{232}+d_9$	10 to 21	8 to 15
$U^{235}+d_{14}$	0	0
$U^{235}+d_9$	0	0
$U^{235}+\alpha_{25}$	0	8
$U^{238}+\alpha_{25}$	>0[c]	>0[c]
$Th^{232}+\alpha_{25}$	>0[c]	>0[c]

[a] Normalized to mass 88.
[b] The subscript on d or α indicates the incident energy in Mev.
[c] See text, Sec. III-C.

neutron fission of U^{235} have been used to construct the fission yield curve shown in Fig. 8. Yields have been accurately measured at each mass number, and presumably represent the true fission-yield curve. The data are mostly mass spectrometric determinations of Petruska *et al.*,[12] with the mass 81 and 82 points taken from Coryell and Sugarman,[1] and the mass 89 value from the work of Reed and Turkevich.[32] The fine-structure which appears in the mass region 84–88 is believed to be an effect of chain branching, brought about by delayed neutron emission[10–12] from As^{85} and Br^{87}.

The mass-yield ratios determined in the present work have been normalized to the fission-yield curve at mass number 88, and the resulting yields for the mass 85 and mass 87 chains are shown as circles in Fig. 8. As compared with the mass spectrometrically determined fission yields of Petruska *et al.*,[12] our mass 85 value is in good agreement, whereas our result at mass 87 is 6% low. This latter deviation exceeds the limit of precision of our replicate experiments by several per cent, and may reflect more meaningfully the uncertainties in our measurements.

E. Discussion

We present in Table V a summary of the fine-structure evidence for the fission reactions which we have studied. The extent of our agreement with published values for thermal neutron fission of U^{235} (see Fig. 8) would imply that our results are probably good to 5%. The deviations in yields at masses 85 and 87 presented in Table V assume a knowledge of a general smooth relation between logarithm of yield and mass number against which variations in the ratios Y_{85}/Y_{88} and Y_{87}/Y_{88} for different types of fission can be seen. However, the reliability of the relative yields of the krypton isotopes studied here exceeds in many cases the reliability of the smooth curves. In particular, positive deviations would be lowered if more curvature exists than shown in Figs. 5 through 7(c), as has been discussed in the comparison for deuteron fission of Th^{232}. Positive deviations for both mass numbers are shown in Table V for deuteron fission of Th^{232} and alpha-particle fission of Th^{232} and U^{238} and for $A=87$ alone for alpha-particle fission of U^{235}. The deviations can alternatively be interpreted largely as an unexpectedly low yield for mass chain 88.

It does not seem likely that our results can be interpreted as a closed shell effect at 50 neutrons, since the deuteron reactions with U^{235} and U^{238} seemed to give normal krypton yields at 14.0 and 9.3 Mev. Any influence of enhanced nuclear stability would be expected to show up systematically in all the fission reactions we have investigated. The absence of low yields for mass numbers 85 and 87, as compared to the thermal neutron fission of U^{235} (Fig. 8), may be related to the expected diminished yields of the delayed neutron emitters As^{85} and Br^{87} at the higher bombarding energies we have employed. Neutron emission is also known[17] to occur following the β decay of Br^{88}, Br^{89}, and Br^{90}, but the resulting effects of chain branching at these mass numbers are not well known.

Wanless and Thode[10] and Fleming, Tomlinson, and Thode[11] have measured the krypton yields in the mass region 83 to 86 for low-energy neutron fission of U^{233}, U^{235}, and U^{238}. The yield of Kr^{84} was found to be high and the deviation from a smooth curve increased slowly with the mass number of the fissioning nucleus. The Kr^{85} yield was high in U^{233} fission, about normal in U^{235} fission, and markedly low in U^{238} fission. These

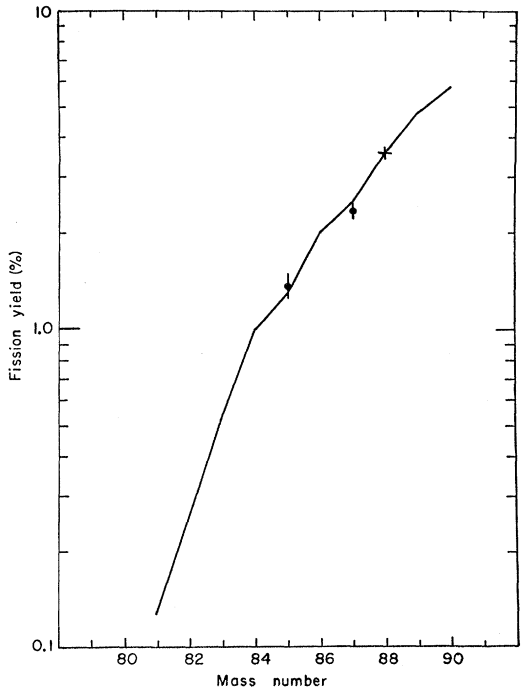

FIG 8. Yield-mass curve for thermal neutron fission of U^{235}. Solid line constructed from data described in the text. × Point of normalization. ● This work.

[32] G. Reed and A. Turkevich, Phys. Rev. **92**, 1473 (1953).

deviations were noted relative to a straight line through the mass 83 and mass 86 yields, and no explanation has been advanced which will satisfy the data for all three fission reactions.

The present study gives a similar close look at relative yields of masses 85, 87, and 88 in a group of fission reactions where the compound nuclei vary from Pa^{234} to Pu^{242}, but where the excitation energies are all close to 20 Mev (about 22 Mev for 14-Mev deuterons, 17 Mev for 9-Mev deuterons, and 20 Mev for 25-Mev alpha particles). Shifts in yields due to delayed neutron emission are expected to be less for the shorter chains involved here compared to those in low-energy neutron fission. No general explanation is apparent for the deviations shown in Table V, but improved knowledge of the course of the yield-mass curve in nearby regions may lead to further interpretation.

ACKNOWLEDGMENTS

We would like to thank Earle White, Frank Fay, and Bill Carrasco of the M.I.T. cyclotron staff for the numerous short bombardments, and the operating crew of the M.I.T. reactor for their cooperation in obtaining the thermal neutron irradiations. We are also grateful to Frank Carter and James A. Kafalas of the Lincoln Laboratory for their valuable suggestions in the design of the experimental apparatus, and to Emil DeAgazio and Henry Zufelt for assistance with the electronic equipment.

APPENDIX I. CALCULATION OF COUNTING EFFICIENCIES

To obtain the experimental results described above, it was necessary to know the relative counting efficiencies of the various species detected by the counter. By the arguments given in Sec. III(A), we have taken the counting efficiencies of Kr^{87}, Kr^{88}, and the β decay of Kr^{85m} to be equal to 1.000. We consider the branching decay of Kr^{85m} and the counting efficiency of Rb^{88} in detail below.

Kr^{85m}

The decay of Kr^{85m} proceeds 77% by β emission to states in Rb^{85} and 23% by isomeric transition[21] to the ground state of Kr^{85}. For the latter transition, the K-shell internal conversion coefficient is 0.41 and the ratio of K-shell conversion to that from the L plus M shells is 6.2.[21] Taking the counting efficiency of the internal conversion electrons to be 1.000, we may calculate the fraction of the isomeric transitions which will contribute to the observed counting rate:

$$e_K+e_L+e_M=(7.2/6.2)e_K,$$
$$(e_K+e_L+e_M)/\gamma=(7.2/6.2)e_K/\gamma=0.47,$$
$$(e_K+e_L+e_M+\gamma)/\gamma=1.47,$$
$$\gamma/(e_K+e_L+e_M+\gamma)=1/1.47=0.68,$$
$$(e_K+e_L+e_M)/(e_K+e_L+e_M+\gamma)$$
$$=1-\gamma/(e_K+e_L+e_M+\gamma)=1-0.68=0.32.$$

Thus of the isomeric transitions, 32% are counted due to internal conversion. The remaining 68% are not detected to any significant extent, as the counting efficiency for 300-kev γ rays in our counter is about 0.003. Since the isomeric transitions comprise 23% of the decays of Kr^{85m}, we have 68% of 23% or 16% of the total decays are not counted. Therefore, the over-all relative counting efficiency for Kr^{85m} is 1–0.16 or 0.84.

Consequently, the observed Kr^{85m} counting rates have been multiplied by the factor 1/0.84 or 1.19 to obtain the relative disintegration rates.

Rb^{88}

The rubidium atoms formed by decay of the parent krypton are deposited on the wall of the counter and remain there. When the radioactive Rb^{88} undergoes β decay, there is equal probability for the β ray to be emitted into the counter and into the wall. If emission is inwards, the β ray will be counted, and as a first approximation we assume that if emission is outwards (into the wall), the decay is not detected. This results in a counting efficiency of 0.500 relative to that for the gaseous krypton species.

To improve upon this value, we consider the effects of backscattering of the β rays by the wall of the counter. For the high-energy β rays emitted by Rb^{88}, no other process is likely to be of importance. As the thickness of the counter wall was sufficient to achieve saturation backscattering conditions, we have used the experimental data of Engelkemeir and co-workers[33] which relates the amount of backscattering to the atomic number of the backscatterer and the maximum energy of the β rays. From these curves and an average Z for brass of 29.3, we find that the ratio of observed counting rates with and without backscatterer is 1.570.

Multiplying our first approximation for the counting efficiency of Rb^{88} by the contribution due to backscattering, we obtain $0.500\times1.570=0.758$. This is the value which has been used in the analysis of our experimental decay curves.

[33] D. W. Engelkemeir, J. A. Seiler, E. P. Steinberg, L. Winsberg, and T. B. Novey, Paper 5 in reference 1.